LA-UR-95- 967

Conf-9503124--1

Los Alamos National Laboratory is operated by the University of California for the United States Department of Energy under contract W-7405-ENG-36.

TITLE: Dynamics of Current Driven Disordered Josephson Junction Arrays

AUTHOR(S): Daniel Dominguez
Niels Grønbech-Jensen
Alan R. Bishop

SUBMITTED TO: Proceedings of the Workshop on "Macroscopic quantum phenomena and coherence in superconducting networks" Frascati, France, March 1-5, 1995

By acceptance of this article, the publisher recognized that the U S Government retains a nonexclusive, royalty-free license to publish or reproduce the published form of this contribution or to allow others to do so for U S Government purposes.

The Los Alamos National Laboratory requests that the publisher identify this article as work performed under the auspices of the U S Department of Energy.

Los Alamos

Los Alamos National Laboratory
Los Alamos, New Mexico 87545

FORM NO. 836 R4
ST. NO. 2629 5/81

MASTER

DISTRIBUTION OF THIS DOCUMENT IS UNLIMITED

DISCLAIMER

Portions of this document may be illegible in electronic image products. Images are produced from the best available original document.

DYNAMICS OF CURRENT DRIVEN DISORDERED JOSEPHSON JUNCTION ARRAYS

DANIEL DOMÍNGUEZ, NIELS GRØNBECH-JENSEN and ALAN R. BISHOP
Los Alamos National Laboratory, Theoretical Division, MS B262
Los Alamos, NM 87545, USA

ABSTRACT

We present dynamical simulations of disordered Josephson junction arrays with a bias current. We study the IV characteristics and vortex dynamics as a function of integer frustration $f = n$, weak frustration $f = n+\delta$ ($\delta \ll 1$) and full frustration $f = n + 1/2$. We study the critical dynamics of vortices and vortex-antivortex pairs close to the critical current i_c. We focus on the study of the plastic flow of vortices ($f = n + \delta$), of vortex-antivortex pairs ($f = n$), and the dynamics of domain walls ($f = n + 1/2$) close to i_c. We analyze the voltage noise and vortex fluctuations in the plastic flow regimes. We obtain the phase diagram for the different dynamical regimes as a function of disorder and applied current. We also study the dynamical critical behavior of depinning close to i_c in the gauge glass limit of the model, $f \to \infty$, calculating critical exponents for the voltage onset and voltage fluctuations. We discuss our results within the context of present theories of the non-linear dynamics of disordered media.

1. Introduction

Two dimensional Josephson junction arrays (JJA) can be designed with very specific geometries and properties. In particular, experiments in JJA with controlled disorder have been done in the past [1], mainly directed to the study of the effects of randomness in the Kosterlitz-Thouless phase transition [2]. Also recently, the study of the JJA as dynamical systems with a large number of coupled degrees of freedom has become of great interest [3,4,5,6,7]. The non-linear dynamics of disordered media driven by an external force F leads to critical phenomena in a great variety of systems [8,9,10]. The interplay between the interactions of a large number of degrees of freedom and a random static potential originates a critical onset of motion with velocity v, following $v \sim (F - F_T)^\zeta$ above a threshold force F_T. Two types of behavior can be distinguished [8]: "elastic flow", where the elastic medium distorts but does not break, and the time averaged flow is homogeneous in space; and "plastic flow", where the motion breaks up into channels and therefore the flow is intrinsically inhomogeneous [10]. A related problem is the onset of flux flow in Type II superconductors [11,12]. It has been shown that close to the critical current, the dissipation starts through channels of plastic vortex flow [11]. Recently, Bhattacharya and Higgins [12] have done experiments in layered superconductors, obtaining a phase diagram for plastic vortex flow as a function of effective pinning strength and current.

In this contribution, we review our present work on the dynamics of disordered

JJA [13,14,15], as a new example of these phenomena [8,9,10]. In this case the driving force is the external current I, and thus the threshold corresponds to the critical current I_c, and the average voltage V is a measure of the motion in the JJA.

2. Dynamical Equations

We consider current driven two dimensional JJA made of $N \times N$ sites in a square lattice, with a the lattice constant. We study their dynamics [3,4,5] using the resistively shunted junction (RSJ) model for the Josephson junctions. The current $I_\mu(r)$, along the μ direction between the superconducting islands at sites r and $r+\mu$, with $\mu = \hat{e}_x, \hat{e}_y$, in the zero temperature classical limit is given by

$$I_\mu(r) = I_0 \sin(\Delta_\mu \theta(r) - A_\mu(r)) + \frac{\Phi_0}{2\pi\mathcal{R}} \frac{d}{dt} (\Delta_\mu \theta(r) - A_\mu(r)) , \tag{1}$$

where $\Delta_\mu \theta(r) = \theta(r+\mu) - \theta(r)$, I_0 is the junctions critical current and $\mathcal{R}$ is their corresponding shunt resistance. The external magnetic field produces the frustration $f(R) = \frac{\Phi(R)}{\Phi_0}$, with $\Phi(R)$ the magnetic flux in the plaquette R and Φ_0 the quantum of flux, and given by

$$2\pi f(R) = A_x(r) + A_y(r+\hat{e}_x) - A_x(r+\hat{e}_y) - A_y(r) \equiv \Delta_\mu \times A_\mu(R), \tag{2}$$

where the link variable is $A_\mu(r) = \frac{2\pi}{\phi_0} \int_r^{r+\mu} \vec{A} \cdot d\vec{l}$. Here, we are neglecting the screening currents by assuming that $A_\mu(r)$ is fully determined by the external magnetic field H. This assumption is correct if the magnetic penetration depth $\lambda \gg Na$ [7]. For the same reason, $\frac{dA_\mu}{dt}$ can be dropped from Eq. (1) since the magnetic field is constant in time. Eq. (1) together with Kirchoff's current conservation law,

$$\Delta_\mu \cdot I_\mu(r) = I_x(r) - I_x(r-x) + I_y(r) - I_y(r-y) = I^{ext}(r), \tag{3}$$

valid at each node, fully define the evolution of the phase $\theta(r,t)$ as a function of time. Here $I^{ext}(r)$ denotes the external current injected at site r. The explicit expression for $\frac{d\theta}{dt}$ derived from these equations is [4]

$$\frac{d\theta(r,t)}{dt} = -\frac{2\pi\mathcal{R}}{\Phi_0} \sum_{r'} G(r,r') \left\{ I^{ext}(r) - \Delta_\mu \cdot [I_0 \sin(\Delta_\mu \theta(r',t) - A_\mu(r'))] \right\}, \tag{4}$$

with $G(r,r')$ being the two-dimensional lattice Green function which depends on the boundary conditions chosen. We take periodic boundary conditions along the x-direction and open boundary conditions along the y-direction. At the bottom (top) of the array the external current is injected (taken out) with $I^{ext}(r_y = 0) = I$, ($I^{ext}(r_y = Na) = -I$), and $I^{ext}(\vec{r}) = 0$ otherwise. We evaluate Eq. (4) with an efficient algorithm based on fast Fourier transform and tridiagonalization techniques as in Ref. [4]. The time integration is carried out using a fixed step fourth order Runge-Kutta method. Typical integration steps are $\Delta t = 0.01 - 0.1\tau_J$ ($\tau_J = \frac{\Phi_0}{2\pi\mathcal{R}I_0}$), and the integration is carried out for time intervals of $t = 5000\tau_J$, after a transient of $2000\tau_J$.

When considering disorder, we assume that the relevant effect of randomness is in the fluxes $\Phi(R)$, thus neglecting disorder on I_0 and $\mathcal{R}$. We consider two different cases. (i) Positional disorder: we take random displacements of the sites, $\vec{r}/a = (i+\delta^i, j+\delta^j)$, with i, j integers, and $\delta^{i,j}(\vec{r})$ a random uniform number in $[-\Delta/2, \Delta/2]$. We use the Landau gauge for which $A(\vec{r}, \vec{r}') = -\frac{2\pi H}{\Phi_0}\frac{(r'_x - r_x)(r'_y + r_y)}{2}$, with H the applied magnetic field. Noting that $\langle f(\vec{R})\rangle = Ha^2/\Phi_0 = f$, we will consider here the cases $f = n + p/q$, which for $\Delta = 0$ maps to the problem with rational frustration $f = p/q$. (ii) Gauge glass: in the limit ($f\Delta \to \infty$) we can take each $A_{\hat{\mu}}(\vec{r})$ as a random variable with uniform distribution in $[-\pi, \pi]$ (and thus $\langle f(\vec{R})\rangle = 0$). This corresponds to the gauge glass model (GGM), proposed as a model of the vortex glass transition [16] in disordered type II superconductors.

3. Basic depinning mechanisms

Let us first review the physics of a JJA with a single defect [3,4,17]. We consider a defect where one of the sites is displaced a distance δ from its regular position in the square lattice [4]. (Qualitatively similar results can be seen in defects where junctions are removed from the lattice [3,17]). Only the four $A_\mu(r)$ links connected to the defect site are changed by its presence. For $f = 0$ the defect is absent, integer frustration $f = n$ describes increasing "strengths" of the defect as compared with the $f = 0$ case. The same can be said for $f = n + p/q$ as compared with the $f = p/q$ case. The following basic depinning mechanisms occur depending on the f considered:

(i) *Vortex-antivortex depinning.* For $f = n$, at low currents $I < I_0$ a vortex-antivortex pair (VAP) is nucleated around the defect [3,4]. There is an effective Lorentz force acting on the VAP that tends to break it apart. This happens at a critical current I_c^{VAP} lower than I_0, the critical current of the ordered ($f = 0$) array. It can be shown [14] that for $\delta \ll 1$, $I_c \approx I_0[1 - 2(\pi\delta f)^2]$. This effect is analogous to the decrease of the depairing current in a superconductor due to disorder.

(ii) *Vortex depinning.* For $f = n+1/(N-1)^2$ there is one vortex in the array. In the absence of defects, the depinning current for a single vortex, due to the square lattice potential, is $I_c^{SV} = 0.1 I_0$ as it was shown in Ref. [18]. When a defect is considered, the vortex will be pinned at the defect site, increasing the depinning current [17]. For $\delta \ll 1$ one can estimate[14] that $I_c^{SV} \approx 0.1 I_0[1 + \pi\delta f]$. This effect is analogous to the increase of the critical current in a superconductor due to disorder. This depinning mechanism is also present for $f = n + p/q$ when $p/q \ll 1$, i.e. for low vortex concentrations.

4. Dynamical regimes of vortices in disordered Josephson arrays

We discuss now JJA with positional disorder. We consider the cases of (a) integer frustration $f = n$, (b) dilute vortex arrays $f = n + p/q$ with $p/q \ll 1$, and (c) full frustration $f = n + 1/2$. We calculate as a function of driving current I and effective disorder $W = f\Delta$, the following magnitudes. The average voltage drop distribution $v_y(r) = \overline{v_y(r,t)}$ with $v_y(\vec{r}, t) = \tau_J(\frac{d\theta(\vec{r}+\hat{y})}{dt} - \frac{d\theta(\vec{r})}{dt})$, and $\overline{v}$ the average over

time. The total average voltage is $v = \left\langle \overline{v(t)} \right\rangle = \left\langle \overline{\frac{1}{N_x(N_y-1)} \sum_{\vec{r}} v_y(\vec{r},t)} \right\rangle$, with $\langle v \rangle$ the average over disorder configurations. The distribution of vorticity is given by $n(\vec{R}) = -\Delta_\mu \times \mathrm{nint}[\frac{\theta(\vec{r}+\hat{\mu})-\theta(\vec{r})-A_{\hat{\mu}}(\vec{r})}{2\pi}]$, where $\mathrm{nint}[x]$ is the nearest integer to x. We calculate the average number of vortex temporal fluctuations as $(\delta n_T)^2 = \left\langle \overline{n_T(t)^2} - \overline{n_T(t)}^2 \right\rangle$, with $n_T(t) = \frac{1}{(N-1)^2} \sum_{\vec{R}} n(\vec{R},t)$. The average vorticity satisfies $\left\langle \overline{n_T(t)} \right\rangle = f$, because of vortex number conservation. The average number of vortex excitations is $n_e = \left\langle \overline{n_e(t)} \right\rangle = \left\langle \overline{\frac{1}{(N-1)^2} \sum_{\vec{R}} |n(\vec{R},t) - [f]|} \right\rangle - \{f\}$, with $[f]$ the integer part of f and $\{f\}$ the fractional part of f. Basically n_e counts the number of vortex-antivortex pairs excited in the array, $n_e \approx 2n_{VAP}$.

4.1. Plastic flow of vortex-antivortex pairs

Let us first consider the case of integer frustration $f = n$. For intermediate values of disorder $W \sim 0.2 - 0.5$, the dynamics close to the critical current i_c of the array is as follows. Below and close to i_c there is a pinned phase where there is no dissipation (voltage $v = 0$). Here the the most defective sites (the ones with larger displacements δ) nucleate VAPs. The external current tends to break the pinned VAPs [3,4]. As the current is increased, the VAPs with weaker pinning can be broken, and the freed vortices and antivortices move until they are pinned again in stronger pinning sites. Therefore, after a transient, the VAPs redistribute in the array in a new stable configuration. Close to i_c there are less and less possibilities of redistributing the VAPs, and at i_c the first VAP finds a path along the array without being pinned in any other site. Above i_c dissipation starts and v grows non-linearly. In this regime we find that the now free VAPs move along certain channels of flow in the array, with the number of those channels, and the number of nucleated VAPs, increasing with increasing current. We show an example of this case in Fig. 1(a). We call this phase [13] a "plastic flow" regime, in analogy to what happens in type II superconductors [11,12]. But, since we are considering $f = n$, there is no underlying flux lattice and therefore the plastic flow is not originated by strong deformations in a given vortex lattice as studied for thin films [11]. Instead, the plastic flow is originated by the generation of VAPs which follow an irregular motion in the disordered array [13]. This rather inhomogeneous motion causes fluctuations in the vorticity, $\delta n_T > 0$, since at a given time there is no exact cancellation of vortex and antivortex excitations, because of the lack of reflection symmetry in this case. At higher currents there is a crossover to a regime where $\delta n_T \approx 0$ and the voltage grows linearly with the current. This latter dynamical regime is characterized by a homogeneous flow of vortices and antivortices all over the sample since the number of flow channels has grown until covering all the sample.

4.2. Plastic flow of vortices

If the frustration is $f = n + p/q$ and $p/q \ll 1$ there is a dilute vortex configuration

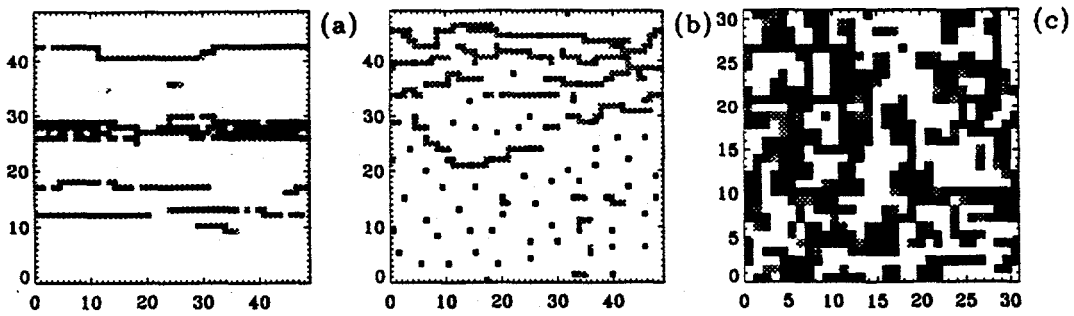

Figure 1: (a) Plastic flow of vortex-antivortex pairs. Black and light grey squares indicate the position of vortices and antivortices respectively, at a given time. Dark grey squares indicate the positions where vortices and antivortices have moved in the past. For a 50×50 array, with $f = 6$, $\Delta = 0.05$, $I = 0.55 I_0$. (b) Plastic flow of vortices. Black squares indicate the position of vortices at a given time. Grey squares indicate the position where vortices have moved in the past. For a 50×50 with $f = 4 + 1/25$, $\Delta = 0.05$, $I = 0.2 I_0$. (c) Plastic flow of domain walls. Plot of the staggered parameter $q(R)$ at a given time (black $q > 0$, white $q < 0$). For a 32×32 array, $f = 3$, $\Delta = 0.1$, $I = 0.23 I_0$.

in the array. We consider [14] for example $p/q = 1/25$ in arrays of size 50×50. For intermediate values of disorder $W \sim 0.2 - 0.5$, the equilibrium configuration of vortices at zero bias $I = 0$ is a random array of vortices, with no crystalline order. (We find that a distorted vortex lattice exists only for very weak disorder $W < 0.1$). Well below the critical current i_c the vortices are pinned by the disorder and there is no dissipation. Close but below i_c some vortices are depinned and move during a transient time until they are pinned again in a new stable configuration. Right at i_c there is at least one vortex that can move without being pinned again. Close but above i_c there are few vortices moving (the others remain pinned) through certain channels of flow. An example [14] of this is shown in Fig. 1(b). As the current is increased further more vortices are moving and therefore more channels of flow are opened. This is a case of plastic flow of vortices, analogous to what has been studied in disordered type II superconductors [11]. There are also fluctuations of the total vorticity here, $\delta n_T > 0$, because of the inhomogeneous flow.

4.3. Plastic flow of domain walls

Probably one of the most interesting problems in JJA is the case of full frustration $f = n + 1/2$ [19]. Here, in the absence of disorder and bias current, the ground state is the so-called "checkerboard" pattern with vortex distribution $n(i,j) = \frac{1}{2}[1 + (-1)^{i+j}]$. Besides VAPs, the other relevant excitations are domain walls separating the two

possible ground states [19]. This can be analyzed by studying the staggered parameter $q(i,j) = (-1)^{i+j}[n(i,j) - 1/2]$, which can take values $\pm 1/2$ for the two possible ground states. Even in the absence of disorder the dynamics of a current driven system is very complex [5], with the motion of current induced domain walls above the critical current. In the weakly disordered case the pinning potential itself induces a random array of pinned domain walls below the critical current i_c. Just above i_c some of the domains remain pinned while others move, originating an inhomogeneous distribution of dissipation and temporal fluctuations of the vorticity $\delta n_T > 0$. This creates a very complex and twisted pattern of domain walls, with part of them pinned and part of them wriggling and flowing. An example [15] of the domain wall pattern, at a given time, is shown in Fig. 1(c).

4.4. IV characteristics

We study here the different dynamical regimes that we can identify in the IV characteristics of the disordered JJA. We discuss first the case of $f = n + 1/25$ in arrays with 50×50 sites. In Fig. 2 we show as a function of bias current $i = I/I_0$ the average voltage v, the voltage temporal fluctuations $(\delta v)^2 = \left\langle \overline{v(t)^2} - \overline{v(t)}^2 \right\rangle$, the vortex fluctuations δn_T, and the number of vortex excitations n_e. We identify the following regimes [14]. (i) *Pinned phase* (PP): the vortex configuration is pinned by the disorder potential. There is no dissipation $v = 0$, no voltage fluctuations $\delta v = 0$, no vortex fluctuations $\delta n_T = 0$, and no vortex excitations $n_e = 0$. (ii) *Plastic vortex flow* (PVF): this is the regime described previously. Above a critical current i_c a few vortices move in channels of flow whereas all the others remain pinned. There is a non-linear onset of voltage v and voltage fluctuations δv. There are also vortex fluctuations $\delta n_T > 0$ but no vortex excitations n_e. The peaks in the behavior of $\delta n_T(I)$ as a function of bias I depend on the disorder configuration chosen, since the particular structure of flow channels is sample dependent [14]. (iii) *Flux flow* (FF): here all the vortices move in the array with the same average velocity. The voltage v grows linearly, i.e. it is a "flux flow" voltage with slope proportional to the vortex concentration p/q, and the voltage fluctuations δv remain approximately constant and low. There are no vortex fluctuations $\delta n_T = 0$ and no vortex excitations $n_e = 0$. The flow is homogeneous in average. (iv) *Plastic vortex-antivortex flow* (PVAF): at high currents, which are close to the single defect I_c^{VAP}, there is a nucleation of vortex-antivortex pairs. The VAPs move in a few channels of flow in the same way as in case of $f = n$ close to i_c. At the same time all the vortices induced by the magnetic field are moving. There is a non-linear increase on v and δv. The flow is again inhomogeneous and there are vortex fluctuations $\delta n_T > 0$. Since there are VAPs, we have that $n_e = 2n_{VAP} > 0$. (v) *Vortex-antivortex flow* (VAF): at very high currents the flow is dominated by the motion of VAPs all over the sample. The voltage increases again linearly, now its slope given by the shunt resistance of the single junctions, and the voltage fluctuations remain constant and about two orders of magnitude larger than in the FF regime. Since the flow is now homogeneous the vortex fluctuations are negligible $\delta n_T \approx 0$. The number of average vortex excitations

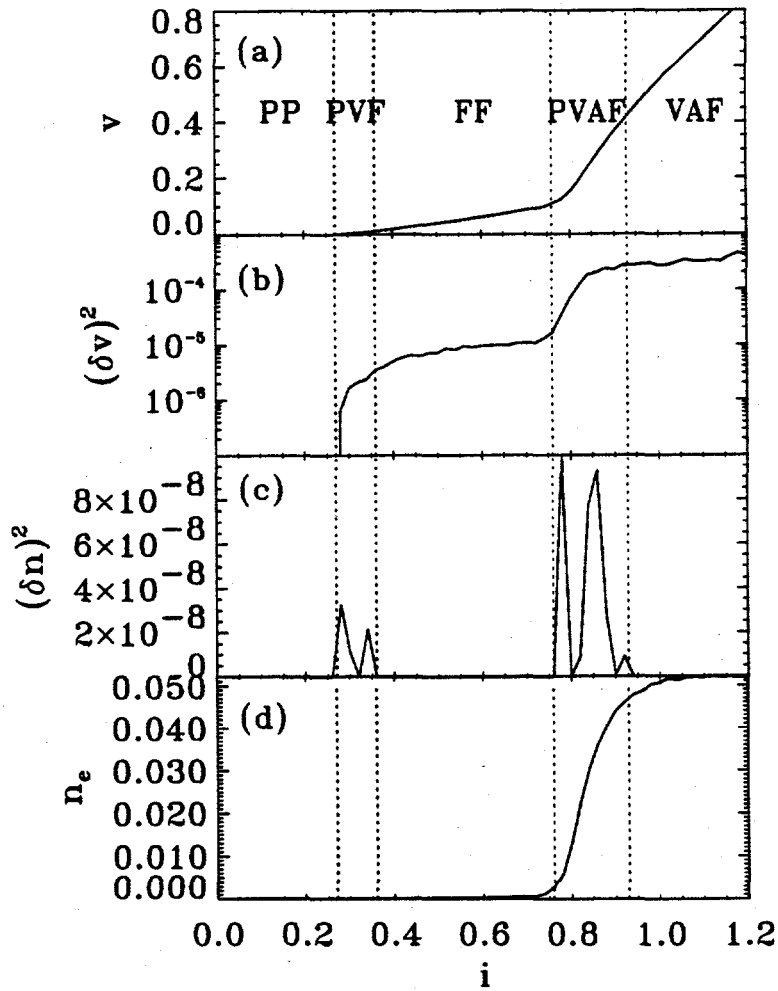

Figure 2: Current biased array with $f = 5 + 1/25$, $\Delta = 0.05$, and 50×50 sites. (a) IV characteristics. (b) Voltage fluctuations $(\delta v)^2$ as a function of $i = I/I_0$. (c) Fluctuations of the total vorticity $(\delta n_T)^2$ as a function of i. (d) Number of vortex excitations n_e as a function of i. PP: pinned phase, PVF: plastic vortex flow, FF: flux flow, PVAF: plastic vortex-antivortex flow, VAF: vortex-antivortex flow.

n_e is independent of I and proportional to W.

In the case of $f = n + 1/2$, the dynamics of domain walls has to be taken into account [15]. In Fig. 3 we show a plot of v, δv, δn_T and the average length of domain walls ℓ, as a function of bias i for a 32×32 array. Above the critical current there is now a plastic domain wall flow (PDWF) where there is a non-linear increase of v and an onset of voltage fluctuations δv as in the other cases. Here we see that the average length ℓ of domain walls is strongly peaked in this regime. This is because the domain walls become strongly twisted and wriggling as a consequence of their plastic motion [15]. Also, due to the inhomogeneous flow, there are fluctuations of vorticity δn_T in this regime.

4.5. Dynamical phase diagrams

In Fig. 4 we show the dynamical phase diagram in the plane $I - W$ showing the different regimes discussed previously. For $f = n$ there are only three regimes [13]: pinned phase, plastic vortex-antivortex flow and vortex-antivortex flow (Fig. 4(a)). We find that for low disorder the critical current follows $i_c \approx i_c^{VAP}$. For very weak disorder we do not see a plastic flow regime, and there is hysteresis around the onset of dissipation (here we only plot the i_c when increasing the current). For $f = n+1/25$ there are the five regimes [14] described previously (Fig. 4(b), we find a similar phase diagram for $f = n + 1/10$). For weak disorder the critical current follows $i_c \approx i_c^{SV}$. Note also that the onset of plastic vortex-antivortex flow approximately coincides with the critical current of the $f = n$ case. For large disorder the two plastic flow regimes merge, being dominated by the flow of VAPs. Also the flux flow regime disappears. In limit of $W \to \infty$ in both cases the dynamics tends to the gauge glass model behavior, with an onset of plastic vortex-antivortex flow at i_c. With increasing f the range in current of the plastic regime saturates for large f, tending to the behavior of the gauge glass.

5. Gauge glass limit and critical dynamics

Finally, we analyze the critical behavior above i_c for the gauge glass model [13]. Here the onset of vortex-antivortex plastic flow is a dynamical critical phenomenon, characterized by two correlation lengths. These are the typical distance between flow channels $\xi_{||}$, and the typical distance between channel splits $\xi_{\perp}$. Both diverge when approaching i_c from above, leaving only one channel close to i_c when $\xi_{||}, \xi_{\perp} > N$. This can be seen in Fig. 5(a)-(c) where we plot the time averaged voltage $v_y(\vec{r})$ for samples of different sizes under the same bias current. In the junctions where VAPs have moved $v_y(\vec{r}) \neq 0$ whereas in the others $v_y(\vec{r}) = 0$. We see that whereas for small samples there is only one channel of flow, after increasing the sample size for a given current, more new channels and channel splitting are evidenced. Furthermore, when increasing the current away from i_c the number of channels and channel splits grow with the bias current. This is shown in Fig. 5(d)-(f). For large currents there is a crossover to homogeneous flow when $\xi_{||}, \xi_{\perp} \approx a$. We have done a detailed study

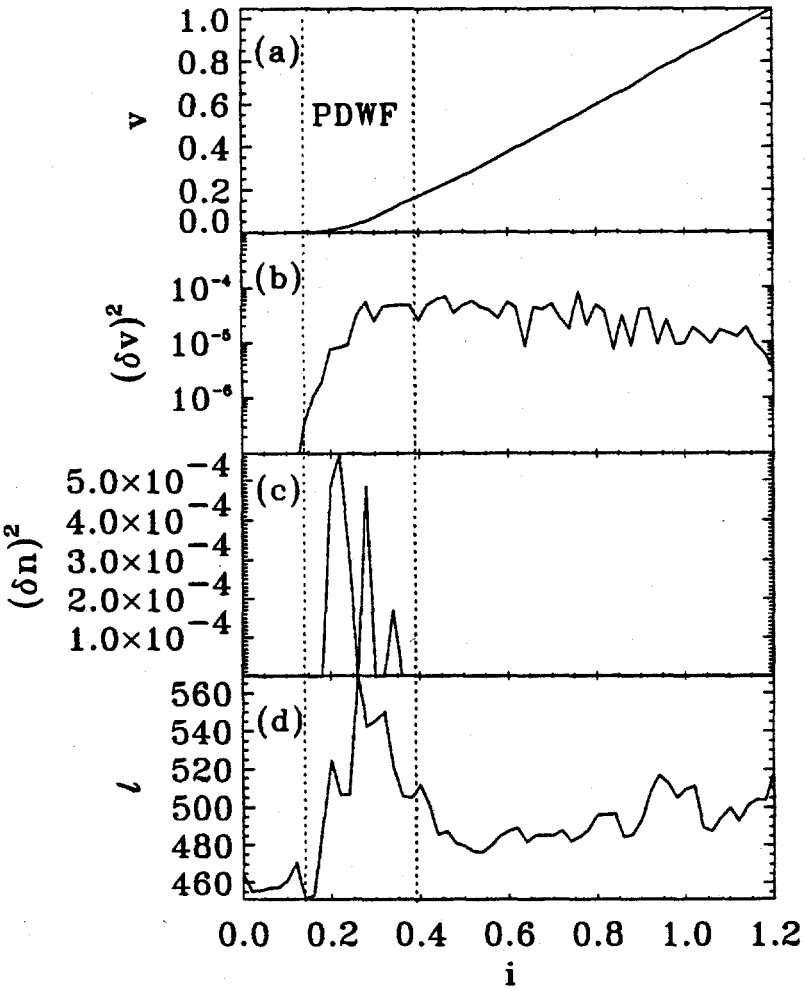

Figure 3: Current biased array with $f = 5 + 1/2$, $\Delta = 0.05$, and 32×32 sites. (a) IV characteristics. (b) Voltage fluctuations $(\delta v)^2$ as a function of $i = I/I_0$. (c) Fluctuations of the total vorticity $(\delta n_T)^2$ as a function of i. (d) Average length of domain walls ℓ as a function of i. PDWF: plastic domain walls flow.

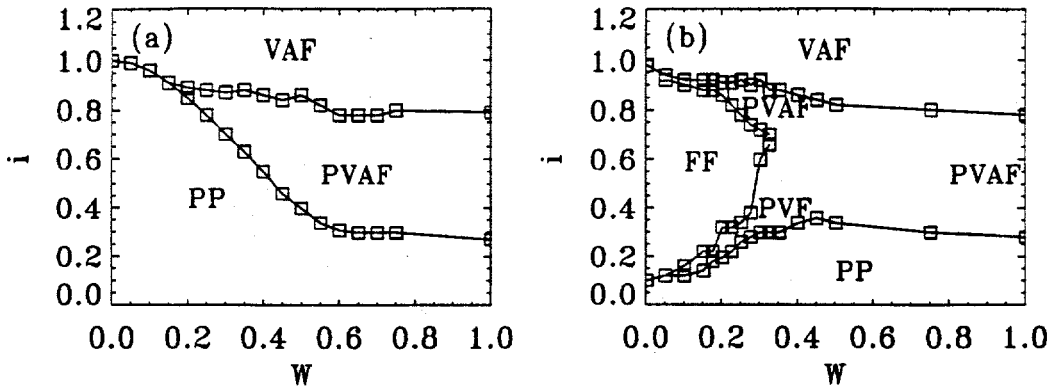

Figure 4: Dynamical phase diagrams of disordered Josephson arrays. Currents bias $i = I/I_0$ vs. effective disorder $W = f\Delta$. (a) For $f = n$, 64×64 arrays. (b) For $f = n + 1/25$, 50×50 arrays. PP: pinned phase, PVF: plastic vortex flow, FF: flux flow, PVAF: plastic vortex-antivortex flow, VAF: vortex-antivortex flow.

of the critical behavior in Ref. [13]. We found that the voltage close to the critical current increases as $v \sim (i - i_c)^{\zeta}$, with $\zeta \approx 2.22 \pm 0.20$. Also above the critical current, there is an onset of voltage temporal fluctuations as $(\delta v)^2 \sim \frac{1}{N^2}(i - i_c^*)^{\psi}$ with $\psi \approx 2.27 \pm 0.20$. Each sample has a well defined threshold current i_c, which is very sensitive to finite size effects and fluctuates from sample to sample for a given size. The sample to sample fluctuations of the critical current, $(\delta i_c)^2 = \langle i_c^2 \rangle - \langle i_c \rangle^2$ follow the power law $\delta i_c \sim N^{-1/\nu_T}$. The exponent ν_T is characteristic of a finite size scaling length $\xi_{FS} \sim (i - i_c)^{-\nu_T}$, which characterizes the distribution of properties in ensembles of samples as a function of their size [9]; and $\nu_T \geq 2/d$. We find $\nu_T \approx 1.09 \pm 0.13$, which is very close to the value found in charge density wave systems [9]. If a one vortex description were valid, the voltage fluctuations would be given by $(\frac{\delta v}{v})^2 \sim \xi^{-(d-4+\eta)}(\xi/N)^d$ with the prefactor $\xi^{-(d-4+\eta)}$ coming from incoherence within a correlation volume, and $d - 4 + \eta > 0$ [8,9]. However, since the long range vortex-vortex interactions play a major role in this case, this may not be correct. In fact, one gets $4 - \eta = (2\zeta - \psi)/\nu_T = 1.99 \pm 0.24 \approx d$, which means that coherence within a correlation volume is relevant.

6. Conclusions

In conclusion, we have shown that the onset of dissipation in disordered JJA occurs always following an inhomogeneous pattern of "plastic flow". Depending on the kind of frustration considered, this involves the motion of vortex-antivortex pairs ($f = n$), vortices ($f = n + p/q$, and $p/q \ll 1$) or domain walls ($f = n + 1/2$). We have given a dynamical phase diagram as a function of disorder and current range of the plastic flow regimes. In the gauge glass limit of strong disorder, the relevant process is the plastic flow of vortex-antivortex excitations, which occur as a critical phenomenon [13]. The plastic flow regimes could be studied in controlled experiments on disordered

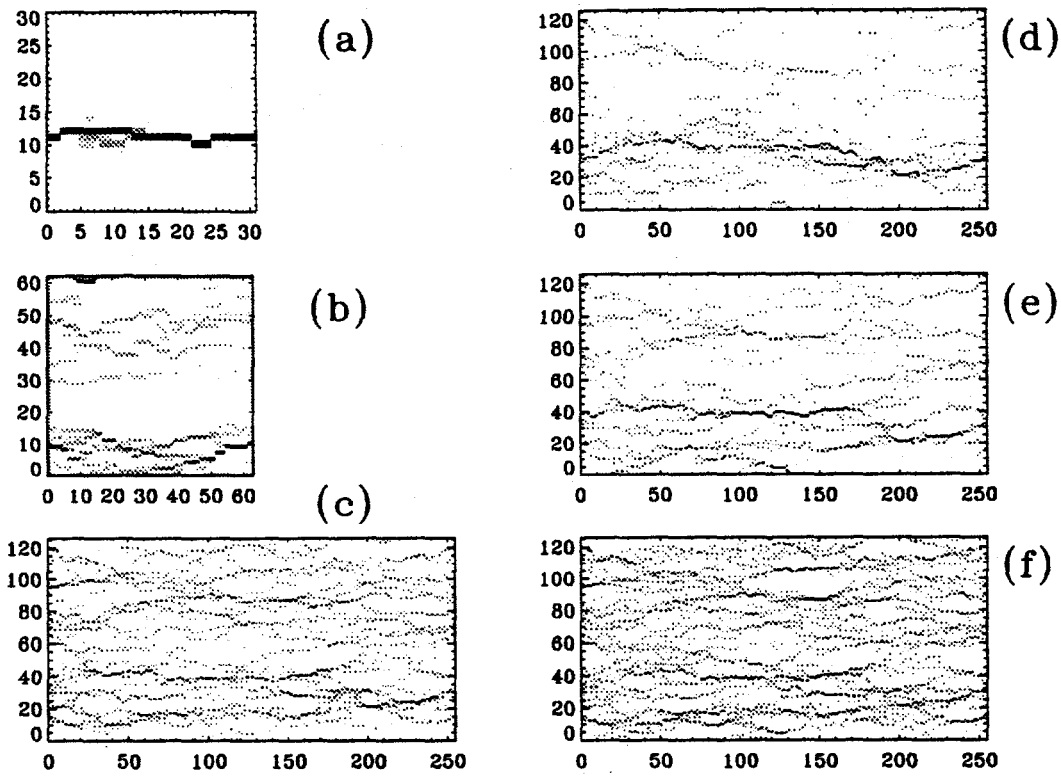

Figure 5: Plot of the time averaged dissipation $v_y(\vec{r})$ showing the sites where vortices and antivortices have moved. Grey scale: black $\equiv$ maximum v_y, white $\equiv v_y = 0$. For the gauge glass model. With bias current $I = 0.255 I_0$ and different sizes: (a) 32×32, (b) 64×64, (c) 256×128. For a given size 256×128 and increasing bias current: (d) $I = 0.22 I_0$; (e) $I = 0.24 I_0$; (f) $I = 0.275 I_0$, (the critical current is $I_c = 0.215 I_0$).

DISCLAIMER

This report was prepared as an account of work sponsored by an agency of the United States Government. Neither the United States Government nor any agency thereof, nor any of their employees, makes any warranty, express or implied, or assumes any legal liability or responsibility for the accuracy, completeness, or usefulness of any information, apparatus, product, or process disclosed, or represents that its use would not infringe privately owned rights. Reference herein to any specific commercial product, process, or service by trade name, trademark, manufacturer, or otherwise does not necessarily constitute or imply its endorsement, recommendation, or favoring by the United States Government or any agency thereof. The views and opinions of authors expressed herein do not necessarily state or reflect those of the United States Government or any agency thereof.

JJA at low temperatures using recently developed vortex imaging techniques [20].

References

1. M. G. Forrester *et al.*, *Phys. Rev. B* **37**, 5966 (1988); D. C. Harris *et al.*, *Phys. Rev. Lett.* **67**, 3606 (1991).
2. E. Granato and J. M. Kosterlitz, *Phys. Rev. B* **33**, 6533 (1986); A. Chakrabarty and C. Dasgupta, *ibid.* **37**, 7557 (1988); M. G. Forrester *et al.*, *ibid.* **41**, 8749 (1990); S. E. Korshunov, *ibid.* **48**, 1124 (1993).
3. W. Xia and P. L. Leath, *Phys. Rev. Lett.* **63**, 1428 (1989); P. L. Leath and W. Xia, *Phys. Rev. B* **44**, 9619 (1991).
4. D. Domínguez *et al*, *Phys. Rev. Lett.* **67**, 2367 (1991); D. Domínguez and J. V. José, *Phys. Rev. B* **48**, 13717 (1993) and *Int. J. Mod. Phys. B* **8**, 3749 (1994).
5. F. Falo *et al*, *Phys. Rev. B* **41**, 10983 (1990); N. Grønbech-Jensen *et al*, *Phys. Rev. B* **45**, 10139 (1992) and *Phys. Rev. B* **46**, 11149 (1992).
6. R. Mehrotra and S. R. Shenoy, *Europhys. Lett.* **9**, 11 (1989); D. Domínguez and H. A. Cerdeira, *Phys. Rev. Lett.* **71**, 3359 (1993), and Phys. Lett. A (1995).
7. D. Domínguez and J. V. José, *Phys. Rev. Lett.* **69**, 514 (1992); see also A. Majhofer *et al*, *Phys. Rev. B* **44**, 9634 (1991); J. R. Phillips *et al*, *Phys. Rev. B* **47**, 5219 (1993).
8. D. S. Fisher, *Phys. Rev. Lett.* **50**, 1486 (1983); and in *Nonlinearity in Condensed Matter*, edited by A. R. Bishop *et al.* (Springer-Verlag, New York, 1987).
9. O. Narayan and D. S. Fisher, *Phys. Rev. Lett.* **68**, 3615 (1992); N. Martys *et al.*, *Phys. Rev. Lett.* **66**, 1058 (1991); M. Dong *et al.*, *Phys. Rev. Lett.* **70**, 662 (1993); A. A. Middleton and N. S. Wingren, *Phys. Rev. Lett.* **71**, 3298 (1993).
10. O. Narayan and D. S. Fisher, *Phys. Rev. B* **49**, 9469 (1994).
11. H. J. Jensen *et al.*, *Phys. Rev. Lett.* **60**, 1676 (1988); A. C. Shi and A. J. Berlinsky, *Phys. Rev. Lett.* **67**, 1926 (1991).
12. S. Bhattacharya and M. J. Higgins, *Phys. Rev. Lett.* **70**, 2617 (1993).
13. D. Domínguez, *Phys. Rev. Lett.* **72**, 3096 (1994)
14. D. Domínguez, to be published.
15. D. Domínguez, N. Grønbech-Jensen and A. R. Bishop, to be published.
16. D. A. Huse and S. Seung, Phys. Rev. B **42**, 1059 (1990); M. P. A. Fisher *et al.*, Phys. Rev. Lett. **66**, 2931 (1991); Y. H. Li, Phys. Rev. Lett. **69**, 1819 (1992).
17. M. B. Cohn *et al*, *Phys. Rev. B* **43**, 12823 (1991).
18. C. J. Lobb *et al*, *Phys. Rev. B* **27**, 150 (1983).
19. See for example G. Ramírez-Santiago and J. V. José, *Phys. Rev. B* **49**, 9567 (1994) and references therein.
20. H. D. Hallen *et al.*, *Phys. Rev. Lett.* **71**, 3007 (1993); S. G. Lachenmann *et al*, *Phys. Rev B* **50**, 3158 (1994).